

Strategies for Optimizing Greases to Mitigate Fretting Wear in Rolling Bearings

J. Bosch, and G. L. Doll*

The Timken Engineered Surfaces Laboratories, The University of Akron, Akron, OH 44325

* Corresponding author: Gary L. Doll, Email: gd27@uakron.edu

ABSTRACT

Strategies for optimizing greases to mitigate fretting wear in grease lubricated rolling bearings are proposed and evaluated. This study is motivated by previous findings where some solid additives in oils were found to reduce fretting wear of bearings via the formation of tribofilms on the rolling elements and raceways. Furthermore, previously reported data explored the effect of enhanced oil bleed on fretting wear in a narrow range of grease base oil viscosities. The scope of this study consists of an evaluation of oil bleed and the incorporation of oxide nanoparticles in a wide range of base oil greases to mitigate fretting wear of rolling element bearings. Grease characterization tests showed that top treated additives did not affect the rheological properties of the greases. Tribological tests showed that enhanced oil content (i.e., bleed) helped mitigate fretting wear in rotational motion. In addition, mitigation of fretting wear in translational and rotational motion was observed for copper oxide (CuO) nanoparticles. This protection was proved via elemental analysis that evidenced the presence of Cu in the surface of the wear scars in both types of tests. Thus, the most effective mitigation strategy found in this study was the incorporation of CuO nanoparticles to the grease.

1. INTRODUCTION

Greases are ubiquitously utilized in sealed rolling element bearings. In these systems, adequate lubricant films are usually generated between the rolling elements and the raceways while the bearing undergoes continuous rotation. Unfortunately, interruptions of this regime may occur. During these periods, intimate contact between the asperities on the rolling elements and the raceways can occur. If the stationary bearing is subjected to vibrations or low amplitude oscillations, fretting wear or false brinelling may occur on the raceways. Fretting wear can be divided according to whether the oscillations are translational or rotational. Each motion will be dominated by different mechanisms, as previous data has reported [1]. For this wear to be considered as fretting, the amplitude of the oscillations must be smaller than the width of the contact area.

However, there is a lack of agreement in the definition of fretting wear and the types of damage it produces in the literature [2]. For instance, Waterhouse describes as fretting damage as any form of material damage accumulation and fretting wear as the amount of material removed from the surface [3]. In the case of fretting fatigue, it corresponds to the formation of cracks as a result of the cyclic load caused by fretting [3]. Fretting corrosion however, involves a wear process where the dominant role of oxidation accelerates the fretting damage [4]. Other authors like Godfrey defined two types of fretting damage, fretting corrosion associated with dry contacts and false brinelling, associated with lubricated contacts [5]. However, the definition of fretting corrosion was eliminated later when fretting damage was observed in nonmetals and noble metals [6]. The main differences between fretting wear and other types of wear is that, due to the displacement being smaller than the contact area, a region in the contact is never exposed to the environment. As a result, entrapment of wear debris within the contact

region occurs [6, 7]. If the materials in contact are ferrous, the debris consists of various forms of Fe_2O_3 and Fe_3O_4 , acting as hard, abrasive material and promoting wear [4, 8].

Due to the complexity of this phenomena, it has been widely studied in several industrial and engineering applications [9]. It is accepted that different sliding parameters such as displacement, frequency, contact pressure, temperature, surface roughness and hardness of the surfaces in contact play a significant role in the fretting wear performance and the type of damage observed [10–14]. Three different regions have been characterized in tangential movement: stick regime, where the interface is under stick conditions, partial slip, where slip is introduced in an annular slip area and fretting fatigue dominates the process, and gross slip, where the tangential force drops and kinetic motion is experienced between the contact surfaces [15].

Some of the applications where this type of wear is prevalent are wheel bearings of vehicles during rail transport, and pitch and yaw bearings in 1.5 MW wind turbines. Vibration of angular contact ball bearings on passenger vehicles being transported by rail causes low amplitude rotational motion between the balls and the raceways under a static radial load and transient axial loads [16]. These bearings are usually lubricated with a lithium complex, NLGI grade 1-2 grease with a base oil viscosity of about 150 at 40 °C. Vibration and dithering encountered by thrust ball bearings supporting the blades and nacelles of large wind turbines produce low to mid amplitude rotational motion between the balls and the raceways under dynamic radial and axial loads. The pitch bearings of wind turbines are typically lubricated with a lithium complex, NLGI grade 1.5 grease with a 460 cSt base oil viscosity at 40 °C.

Previous research revealed that whereas solid additives, such as boric acid or molybdenum disulfide, are more effective than bleed rate in mitigating translational fretting-type wear, an increased bleed rate was more effective than solid additives if the fretting wear

resulted from rotational oscillations [1, 17]. Recently, it has been reported that nanocrystalline metal oxides such as copper oxide (CuO), zirconium oxide (ZrO), and zirconium dioxide (ZrO₂) can form effective wear-resistant tribo-films when dispersed as an additive in ultra-low viscosity oils [18, 19].

The aim of this NLGI-sponsored research project is to evaluate the ability of these nanocrystalline metal oxides as additives in lithium complex greases to mitigate rotational and translational fretting wear in rolling bearings. To do so, grease characterization tests via cone penetration, bleed rate test and rheology tests were performed. Two tribological tests consisting of a high frequency reciprocating rig, to study translational fretting wear, and a modified Fafnir test, to study rotational fretting wear, were used.

2. EXPERIMENTAL

Three commercially available synthetic lithium complex greases were used in this study with viscosities of 100, 220 and 460 cSt. These greases were selected since they are used in a wide range of applications. Three different nanoparticle oxides were used to study the role played of solid additives in both rotational and translational motions. The oxides selected were CuO with a particle size of 30 nm, ZrO₂ with a particle size of 25 nm, and ZrO with a particle size of 40 nm. Reactive grade CuO and ZrO₂ nanoparticle powders with a purity of 99% were purchased from Alfa Aesar, and ZrO nanoparticle powder was purchased from American Element. To study the effect of the enhanced oil bleeds, synthetic base oils (BO) were added to the greases according to its base viscosity with 1 and 5 wt.% additions. Additives were incorporated to the greases and manually mixed for 1 minute to ensure proper distribution. An automatic mixer was then used to fully mix the greases and the additives for 45 minutes. After mixing, greases were transferred to a sealed container to prevent contamination.

The consistency of the grease was measured using standard cone penetration test in accordance with the ASTM standards D-217 and D-1403 [20, 21]. This test consists of dropping a solid weight with a cone shape into a worked grease sample. The penetration distance of the cone is an indicator of the consistency of the grease. In this study, half size equipment was used, and data were converted to a full-size standard equipment. This procedure can be found in the ASTM D1403 standard [21]. Grease samples were worked for 60 double strokes with a manual standard grease worker.

Standard cone bleed tests were performed according to ASTM D1742 in order to determine the bleed rates of the greases and observe any change in the behavior promoted by the additives [22].

To determine the fretting wear performance of the greases in translational motion, a PCS Instruments High Frequency Reciprocating Rig (HFRR) was used according to the ASTM D7594 standard. The fretting gross slip regime was selected and achieved with a stroke length of 40 μm , a 25 Hz oscillation frequency, a load of 10 N for a total number of cycles of 45,000 [15]. The Hertzian contact pressure was calculated and maintained at 1.4 GPa for all the experiments. The lower and upper specimens in the tribometer were made of hardened 52100 steel and the upper specimen's sphere diameter was 6 mm.

In order to study the effect of the additives in the rotational motion, a modification to the ASTM D4170-16 standard test (also known as Fafnir test) was made [23]. The modified test is essentially the same test as the standard except for the load is applied with an MTS axial torsion load frame. As per machine requirements, the parameters selected do not match the Fafnir test. However, the same energy is dissipated in the contact area compared to the standard test to ensure the same severity is applied to the specimens. Thrust ball bearings from NTN with the part number 0-5 were selected as testing specimens. A load of 18 kN was applied with a

rotation of 3 degrees at 8 Hz oscillation. The test duration was 25 hours for a total number of cycles of 720,000 cycles. This setup showed enhanced reliability in previous studies as it was able to sustain the load more consistently than the standard method [17].

Analysis of the wear data was performed using a scanning white light interferometry (SWLI) microscope, Zygo Newview 7300. The lower and upper specimens from the HFRR tests were studied using this instrument. This allowed for the quantification of the wear volumes from the tribological experiments.

Optical characterization was performed using an optical microscope (OM). Scanning electron microscopy (SEM) characterization and local composition analysis via energy dispersive X-ray spectroscopy (EDX) were performed using a Tescan Lyra 3 XMU microscope. An acceleration voltage of 20 eV and a working distance of 10 mm were used according to the ASTM E986-04 standard [24].

3. RESULTS AND DISCUSSION

Penetration depths for all tested samples and the corresponding NLGI grade are presented in Table 1. Despite the incorporation of different types of additives, the NLGI grade was kept constant. This is not a coincidence as the amount of additive incorporated was targeted to avoid severe modification of the rheological properties of the grease.

Regarding the bleed rates of the greases, Figure 1 presents the normalized bleed rate for grease type. The additives modified the bleed rates of the greases in all cases. In the case of the nanopowder additives, CuO did not severely affect the bleed rates in the case of the 100 cSt grease whereas it partially decreased the bleed rate in the 220 cSt grease and increased the rate it in the 460 cSt grease. ZrO₂ nanoparticles decreased the bleed rate in the lower viscosity

greases and increased the rate in the 460 cSt grease. ZrO nanoparticles severely decreased the bleed rate in all greases, a behavior that will be crucial for the following tests. The decrease in bleed rate may be explained by nanopowders clogging the pores in the grease matrix, thereby reducing the amount of oil that can move freely in and out of the matrix [17]. Regarding the oil additions, bleed rates were always increased as more oil was available. The 460 cSt grease displayed an interesting behavior, Figure 1c shows how this grease displayed the lowest bleed rate. It can be explained via the higher viscosity the base oil has, not being able to flow through the matrix as easily as the other greases.

Rheological tests allowed for the characterization of the flow point of the greases and if the additives significantly modified the rheological properties of the grease. The oscillating procedure gives the storage, G' , and loss, G'' , moduli. The storage modulus is the solid-like response and in-phase with the driving signal. The loss modulus is the viscous response and out-of-phase with the driving signal. This will be important because when the storage and loss moduli cross the nature of the material changes from either a solid-like to viscous or viscous to solid-like material, this point is known as the flow point. The modulus at this cross point is known as crossover modulus. The flow points are presented in Figure 2 for two temperatures, 40°C in black and 80°C in red. The flow point at lower temperature is lower for the higher viscosity greases. However, the crossover modulus of the 100 cSt grease is not affected by the temperature. This can be explained via the lower viscosity of the base oil, allowing it to flow earlier than the rest. Furthermore, the addition of base oil raises the crossover modulus, meaning the flow point occurs earlier. This can be clearly seen in the 100 cSt grease.

Further information of the flow point can be obtained from the oscillatory rheology tests. The crossover stress provides information of the stress required to promote the flow point. Figure 3 presents the crossover stresses for each treated grease. Figure 3 shows that at lower

temperatures a higher stress is required to promote the flow point. This makes sense as the temperature affects the viscosity and as such, the flow point. Based on the results, it can also be seen that oil addition promotes the flow point earlier in the curve. Due to the large variation in the results, it is difficult to extract clear evidence of the process. Interestingly, the effect of the additives on the flow properties are inconclusive, meaning they do not significantly affect the flow properties, something important for our study as it play a crucial role on the wear results.

Wear volume plots are presented in Figure 4 after performing HFFR tests (i.e., translational motion). The volume down is obtained using the Zygo 3D profiler and it accounts for the volume of material removed from the lower specimen. Here it can be seen that in most cases the effect of the additives did not substantially affect the result. There is however an additive that may be affecting the wear resistance. This is the case for CuO nanoparticles, which promoted a lower volume down compared to the baseline in all cases. In translational fretting wear, surface-active agents appear to dominate the process, meaning if CuO tribofilms are formed on the surface, mitigation of fretting wear can be observed.

In the case of the oil additions, there is not a significant effect on the wear volume measurements. This is in accordance with previous data that showed increased oil bleeds do not significantly affect the wear behavior resulting from translational motion [2, 17]. The only trend observed was that 1 wt.% base oil increased the wear volume in the 220 cSt. There is currently no explanation for this observation.

Wear scar depth measurements can be extracted from the tribological test using the Zygo 3D profiler. Wear scar maximum depth is presented in Figure 5. If there is a substantial increase in the wear scar depth, it could be an indicator of agglomeration of the incorporated nanoparticles. As Figure 5 shows, there is not a clear trend on if the solid additives have

severely affected the depths of the wear scars. There is, however, a high variability among the tests, and it can be concluded that neither increased bleed rates nor nanoparticle additives statistically altered the maximum wear depth from wear depths determined for the baseline greases.

Weight loss measurements after the modified Fafnir tests are presented in Figure 6. Overall, the 460 cSt grease provided less wear protection compared to the other greases (see Figure 6c). This is in line with the previous findings, where the main driving factor of rotational fretting wear was the bleed rate of the grease and its ability to flow. This 460 cSt grease displayed the lowest bleed rates as observed in Figure 1. With the powder additives, it was observed that CuO provided some protection for the lower viscosity greases (see Figure 6a, and 6b). In the case of the 460 cSt grease, this trend is not observed and it may be explained by the lower bleed rate of this grease, inhibiting any protective effect generated by the CuO. For the greases with the ZrO₂ additive, higher weight loss was promoted. This may be due to abrasive wear promoted by the particles as well as to the lower bleed rate observed in the bleed rate tests. Similarly, ZrO nanoparticles also promoted higher wear. Furthermore, it was observed that increased oil bleeds significantly enhanced the rotational fretting wear resistance in all cases, results that are in accordance with our hypothesis and previously available data.

Optical micrographs at 10× magnifications of lower specimens tested in HFRR rig are presented in Figure 7 for the 220 cSt grease. It can be seen that there are not substantial differences between the additives, thus illustrating the need for an interferometer to quantify the severity of the fretting damage promoted. The grease containing CuO nanoparticles shows a less severely damaged wear scar. This is in accordance with previous data in Figure 4 where CuO nanoparticles promoted lower wear volumes.

Optical micrographs at 10× magnifications of the thrust bearing raceways after the modified Fafnir test are presented in Figure 8 for the 220 cSt grease. As results in Figure 6 suggest, greases containing CuO nanoparticles promoted less fretting wear damage compared to the baseline. Furthermore, enhanced oil content protected the thrust bearings from fretting wear. It can be observed that greases containing ZrO₂ and ZrO nanoparticles showed the most severely affected surface among all tests. This is in accordance with Figure 6, proving the abrasive wear suggested by the larger particle size as well as increased hardness of the particles. In addition, this enhanced wear damage can be correlated with the lower oil bleed rates observed for these greases.

To understand the fretting wear protection imparted by greases containing CuO nanoparticles, SEM and EDX analysis were performed on both sets of specimens. Figure 9 shows a wear scar of a specimen after an HFRR test for the 100 cSt grease containing CuO nanoparticles. It can be seen that the Cu content increases inside the wear scar, with a maximum content of 0.53 wt.%. This is crucial as in HFRR tests, tribofilms formed via surface-active agents can form during the test and mitigate wear. It has been observed that Cu is reacting with the surface of the metal, mitigating translational fretting wear as was shown in Figure 4 with the decrease in wear volume in all greases.

Surprisingly, greases containing CuO nanoparticles also showed an enhanced protective behavior in the rotational fretting wear tests. As the bleed rate was kept constant, the mitigation effect was suspected to be provided by the reaction of the nanoparticles with the surface. As such, Figure 10 shows SEM and EDX analysis of a wear scar in the raceway of a thrust ball bearing tested in 220 cSt grease containing CuO nanoparticles. It was observed that outside the wear scar, the content of Cu is minimal. However, in the wear scar the content

increased up to 0.58 wt.%. Meaning Cu is reacting with the surface, and the resulting tribofilms appeared to mitigate the rotational fretting wear in all greases.

4. CONCLUSIONS

Based on the results presented in this study, the following conclusions can be drawn about the strategies for optimizing greases to mitigate fretting wear:

- Regarding the properties of the grease, it was found that all greases displayed the same consistency with an NLGI grade of 2. In the case of the bleed rate, it was found that the incorporation of ZrO nanoparticles inhibited the static oil bleed, and also negatively affected the performance in wear tests. To some extent, ZrO₂ nanoparticles also showed a similar behavior. Furthermore, rheology results showed how additives did not severely affect the flow properties of the grease with the exception of oil additions. In that case, the flow point occurred earlier in the curve.
- It was found that CuO nanoparticles additions to the grease mitigated fretting wear from translational motion whereas ZrO and ZrO₂ nanoparticles additions promoted increased wear volumes. The addition of base oil to the greases did not significantly affect the wear volume observed.
- Surprisingly, CuO nanoparticles additions to the grease also mitigated fretting wear from rotational motion whereas ZrO and ZrO₂ promoted higher weight loss. It was found that the addition of 1 wt.% base oil did not significantly affect the fretting wear resistance whereas 5 wt.% protected the bearings.
- The findings for some of the zirconium powder additives in translational motion were not in accordance with the initial hypothesis due to the combination of hardness and large size for the zirconium nanoparticles, which is believed to promote abrasive wear.

In the case of the CuO nanoparticles, due to the ductility, this behavior was not observed. To further explore this behavior, a similar study with ZrO₂ nanoparticles with much smaller sizes (i.e., ~9 nanometers) has been started.

ACKNOWLEDGEMENTS

Authors would like to acknowledge NLGI for their support of this research. Furthermore, authors would like to acknowledge the students and staff at TESL and The University of Akron. The authors especially thank Dr. Paul Shiller for his guidance in the rheological measurements and analysis, Dr. Barbara Fowler and Christian Ondarza for their assistance in the tribological measurements, Mr. Brett Bell for his assistance in the modified Fafnir tests, and Dr. Kuldeep Mistry of the Timken Company for his input and suggestions.

REFERENCES

1. Saatchi A, Shiller PJ, Eghtesadi SA, Liu T, Doll GL. A fundamental study of oil release mechanism in soap and non-soap thickened greases. *Tribol. Int.* **2017**, *110*, 333–40. doi: 10.1016/j.triboint.2017.02.004.
2. Kontou A, Taylor RI, Spikes HA. Effects of dispersant and ZDDP additives on fretting wear. *Tribol. Lett.* **2020**, *69*, 1–13. doi: 10.1007/S11249-020-01379-6.
3. Waterhouse RB. Fretting fatigue. **2013**, *37*, 77–98. doi: 10.1179/IMR.1992.37.1.77.
4. Heitz E. Fretting corrosion. Von R. B. Waterhouse. 253 S. 306 Abb., 13 Tab. 1972, Pergamon Press, Oxford, New York, Toronto, Sydney, Braunschweig. *Geb. Mater. Corros.* **1975**, *26*, 172–3. doi: 10.1002/MACO.19750260224.
5. Godfrey D. Fretting corrosion or false brinelling?. *Tribol. Lubr. Technol.* **2003**, *59*,.
6. Hurricks PL. The mechanism of fretting — A review. *Wear* **1970**, *15*, 389–409. doi:

- 10.1016/0043-1648(70)90235-8.
7. Fouvry S, Liskiewicz T, Kapsa P, Hannel S, Sauger E. An energy description of wear mechanisms and its applications to oscillating sliding contacts. *Wear* **2003**, *255*, 287–98. doi: 10.1016/S0043-1648(03)00117-0.
 8. Varenberg M, Halperin G, Etsion I. Different aspects of the role of wear debris in fretting wear. *Wear* **2002**, *252*, 902–10. doi: 10.1016/S0043-1648(02)00044-3.
 9. Fouvry S, Kapsa P, Vincent L. Analysis of sliding behaviour for fretting loadings: determination of transition criteria. *Wear* **1995**, *185*, 35–46. doi: 10.1016/0043-1648(94)06582-9.
 10. Uhlig HH. Mechanism of fretting corrosion. *J. Appl. Mech.* **1954**, *21*, 401–7. doi: 10.1115/1.4010940.
 11. Uhlig HH, Feng IM, Tierney WD, McClellan A. A fundamental investigation of fretting corrosion **1953**.
 12. Hirsch MR, Neu RW. Temperature-dependent fretting damage of high strength stainless steel sheets. *Wear* **2016**, 6–14. doi: 10.1016/J.WEAR.2015.10.007.
 13. Warmuth AR, Sun W, Shipway PH. The roles of contact conformity, temperature and displacement amplitude on the lubricated fretting wear of a steel-on-steel contact. *R. Soc. Open Sci.* **2015**, *3*,doi: 10.1098/RSOS.150637.
 14. Lu W, Zhang P, Liu X, Zhai W, Zhou M, Luo J, Zeng W, Jiang X. Influence of surface topography on torsional fretting wear under flat-on-flat contact. *Tribol. Int.* **2017**, *109*, 367–72. doi: 10.1016/J.TRIBOINT.2017.01.001.
 15. Vingsbo O, Söderberg S. On fretting maps. *Wear* **1988**, *126*, 131–47. doi: 10.1016/0043-1648(88)90134-2.
 16. Brinji O, Fallahnezhad K, Meehan PA. Analytical model for predicting false brinelling in bearings. *Wear* **2020**, *444–445*, 203135. doi: 10.1016/j.wear.2019.203135.

17. Saatchi A. The effect of grease composition on fretting wear, The University of Akron, **2019**.
18. Demas NG, Erck RA, Lorenzo-Martin C, Ajayi OO, Fenske GR. Experimental evaluation of oxide nanoparticles as friction and wear improvement additives in motor oil. *J. Nanomater.* **2017**, *2017*, 1–12. doi: 10.1155/2017/8425782.
19. Khare HS, Lahouij I, Jackson A, Feng G, Chen Z, Cooper GD, Carpick RW. Nanoscale generation of robust solid films from liquid-dispersed nanoparticles via in situ atomic force microscopy: Growth kinetics and nanomechanical properties. *ACS Appl. Mater. Interfaces* **2018**, *10*, 40335–47. doi: 10.1021/acsami.8b16680.
20. ASTM D217-21, Standard test methods for cone penetration of lubricating grease, ASTM International, West Conshohocken, PA, 2021, www.astm.org.
21. ASTM D1403-20b, Standard test methods for cone penetration of lubricating grease using one-quarter and one-half scale cone equipment, ASTM International, West Conshohocken, PA, 2020, www.astm.org.
22. ASTM D1742-20, Standard test method for oil separation from lubricating grease during storage, ASTM International, West Conshohocken, PA, 2020, www.astm.org.
23. ASTM D4170-6, Standard test method for fretting wear protection by lubricating greases, ASTM International, West Conshohocken, PA, 2003, www.astm.org.
24. ASTM E986-04 Standard practice for scanning electron microscope beam size characterization. West Conshohocken, PA; ASTM International, 2017. <https://doi.org/10.1520/E0986-04R17>.

FIGURE CAPTIONS

Figure 1. Bleed rate results for each commercial lithium grease treated: (a) 100 cSt, (b) 220 cSt, and (c) 460 cSt.

Figure 2. Crossover modulus for each commercial lithium grease treated: (a) 100 cSt, (b) 220 cSt, and (c) 460 cSt.

Figure 3. Crossover stress for each commercial lithium grease treated: (a) 100 cSt, (b) 220 cSt, and (c) 460 cSt.

Figure 4. Wear volume after HFRR test for each commercial lithium grease treated: (a) 100 cSt, (b) 220 cSt, and (c) 460 cSt.

Figure 5. Wear scar maximum depth after HFRR test for each commercial lithium grease treated: (a) 100 cSt, (b) 220 cSt, and (c) 460 cSt.

Figure 6. Weight loss after modified Fafnir test for each commercial lithium grease treated: (a) 100 cSt, (b) 220 cSt, and (c) 460 cSt.

Figure 7. Optical microscopies of lower specimens tested in HFRR rig using 220 cSt grease at 10× magnifications.

Figure 8. Optical microscopies of thrust bearing raceways tested in modified Fafnir rig using 220 cSt grease at 10× magnifications.

Figure 9. SEM and EDX spectra of lower specimen tested in HFRR rig using 100 + CuO grease at 2130× magnifications.

Figure 10. SEM and EDX spectra of thrust bearing raceways tested in modified Fafnir rig using 220 + CuO grease at 140× magnifications.

TABLES

Table 1. Penetration depths recorded for each treated grease.

Grease	Addition	Penetration distance $\frac{1}{2}$ size testing	Penetration distance	NLGI grade
100 cSt	As-received	141.8 \pm 0.9	288.6 \pm 1.8	2
	1% CuO	135.3 \pm 0.4	275.6 \pm 0.8	2
	1% ZrO ₂	138.4 \pm 0.8	281.8 \pm 1.7	2
	1% ZrO	134.3 \pm 0.7	273.6 \pm 1.5	2
	1% Base oil	138 \pm 0.6	281 \pm 1.3	2
	5% Base oil	141.9 \pm 0.5	288.8 \pm 0.9	2
220 cSt	As-received	143.4 \pm 0.3	291.8 \pm 0.5	2
	1% CuO	143 \pm 0.4	291 \pm 0.7	2
	1% ZrO ₂	137.5 \pm 0.7	280 \pm 1.3	2
	1% ZrO	141.8 \pm 0.6	288.6 \pm 1.1	2
	1% Base oil	139.3 \pm 0.7	283.6 \pm 1.4	2
	5% Base oil	143.2 \pm 0.7	291.4 \pm 1.3	2
460 cSt	As-received	140.8 \pm 1.1	286.6 \pm 2.1	2
	1% CuO	138.5 \pm 0.9	282 \pm 1.8	2
	1% ZrO ₂	142.5 \pm 0.8	290 \pm 1.6	2
	1% ZrO	141.7 \pm 0.4	288.4 \pm 0.8	2
	1% Base oil	142 \pm 0.6	289 \pm 1.2	2
	5% Base oil	143.3 \pm 0.3	291.6 \pm 0.5	2

FIGURES

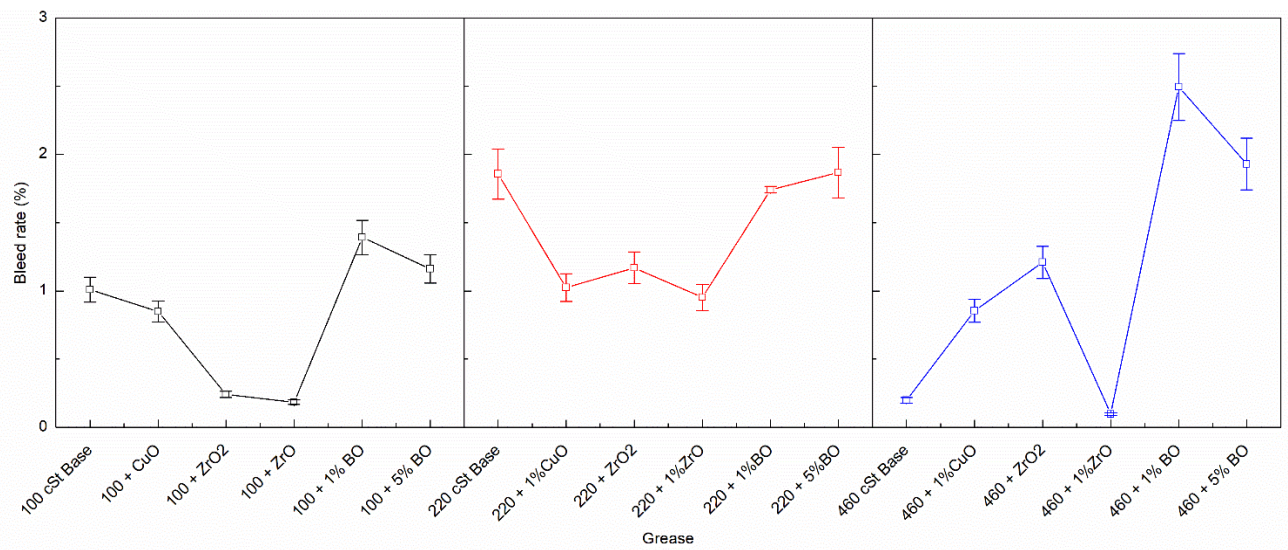


Figure 1. Bleed rate results for each commercial lithium grease treated: (a) 100 cSt, (b) 220 cSt, and (c) 460 cSt.

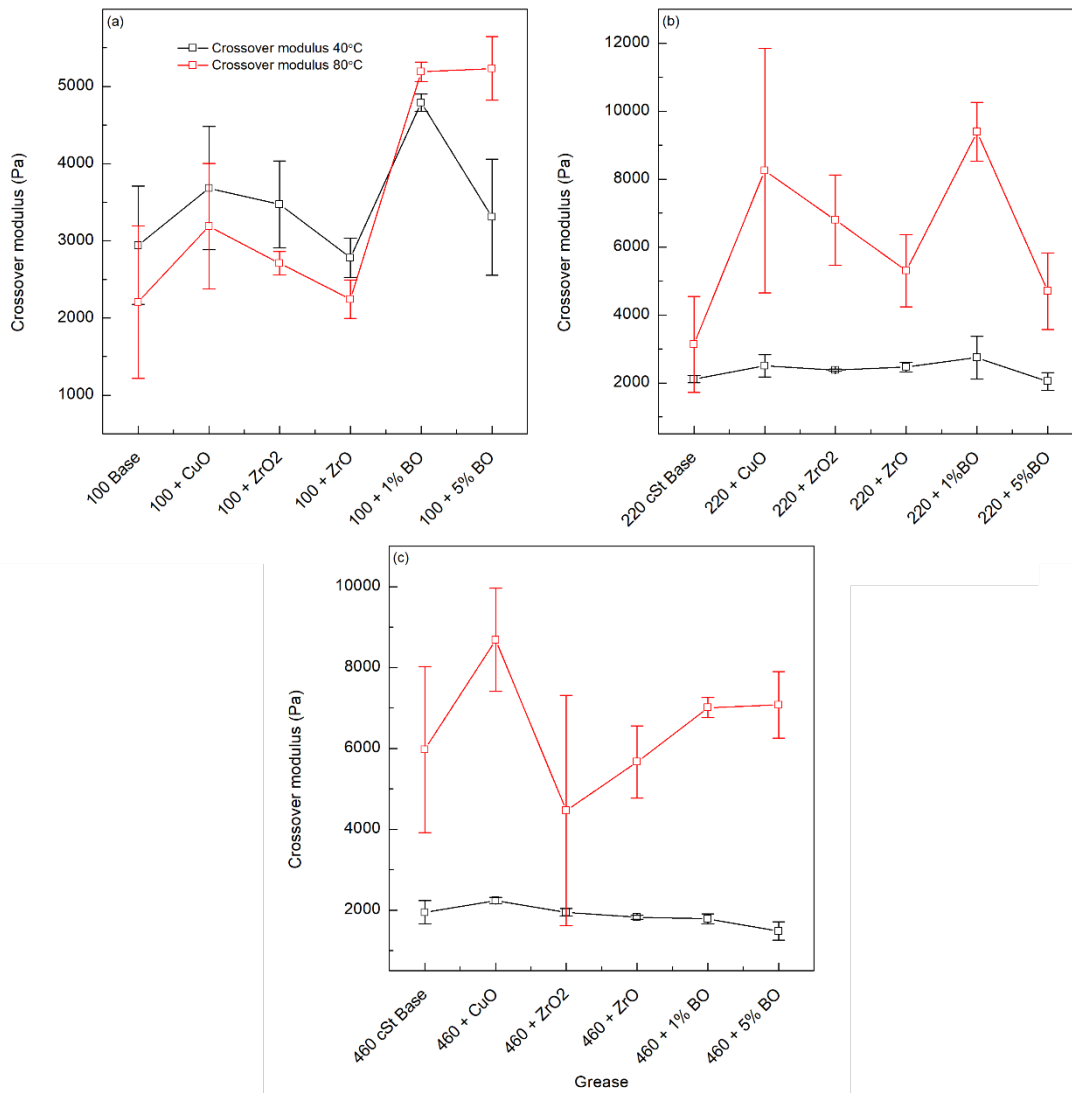


Figure 2. Crossover modulus for each commercial lithium grease treated: (a) 100 cSt, (b) 220 cSt, and (c) 460 cSt.

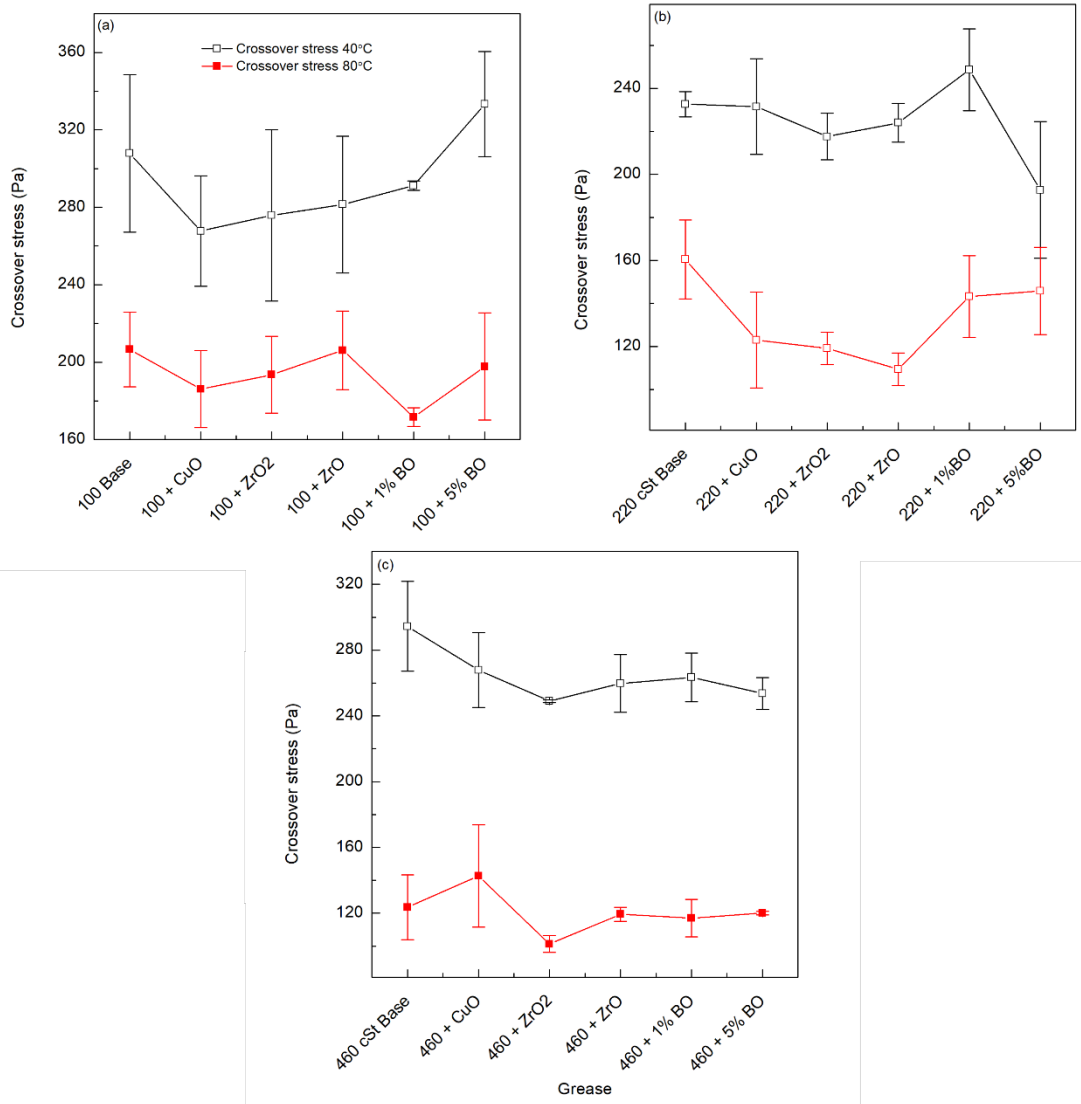


Figure 3. Crossover stress for each commercial lithium grease treated: (a) 100 cSt, (b) 220 cSt, and (c) 460 cSt.

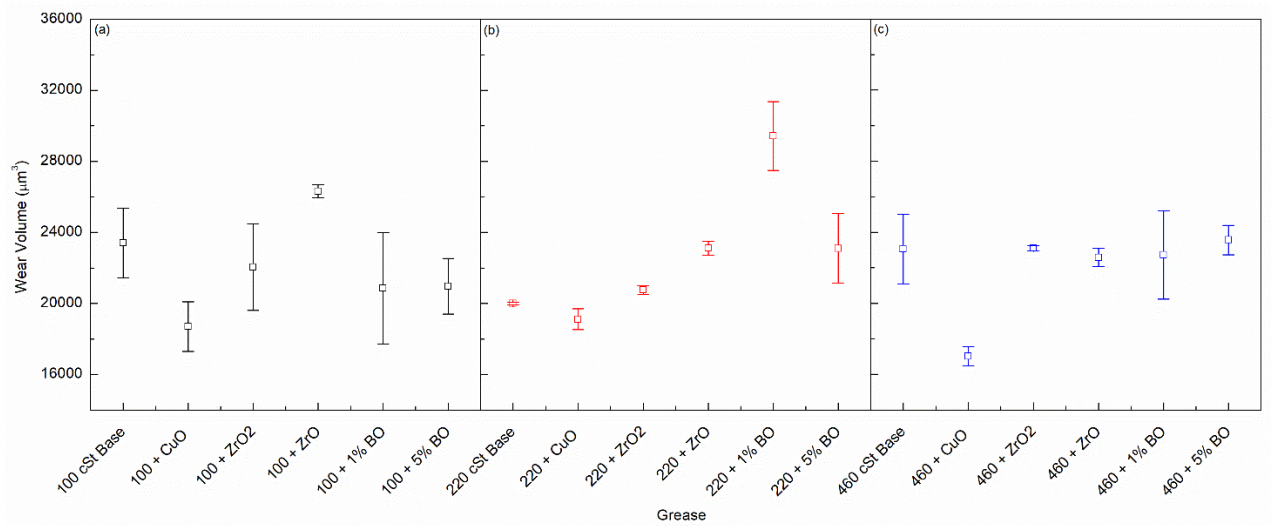


Figure 4. Wear volume after HFRR test for each commercial lithium grease treated: (a) 100 cSt, (b) 220 cSt, and (c) 460 cSt.

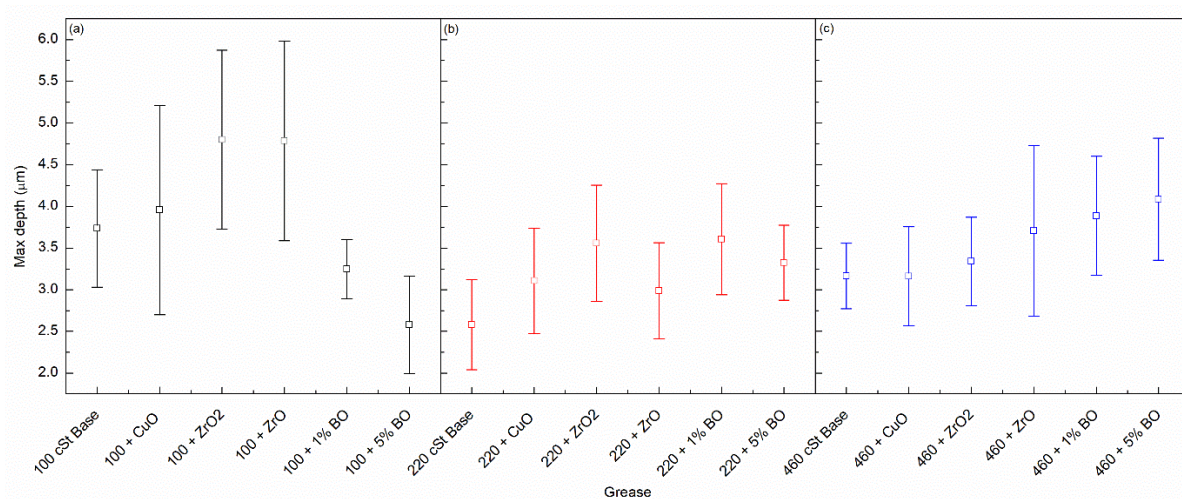


Figure 5. Wear scar maximum depth after HFRR test for each commercial lithium grease treated: (a) 100 cSt, (b) 220 cSt, and (c) 460 cSt.

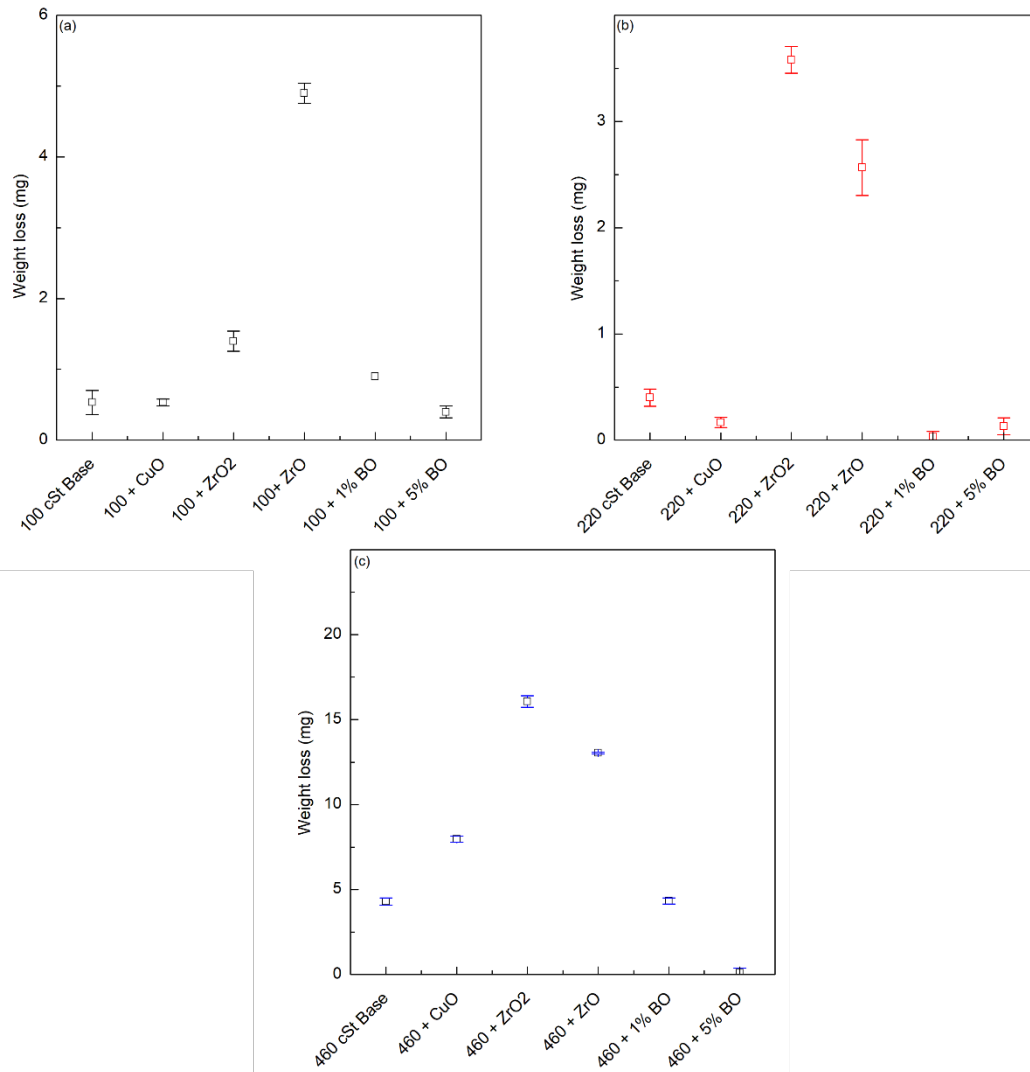


Figure 6. Weight loss after modified Fafnir test for each commercial lithium grease treated: (a) 100 cSt, (b) 220 cSt, and (c) 460 cSt.

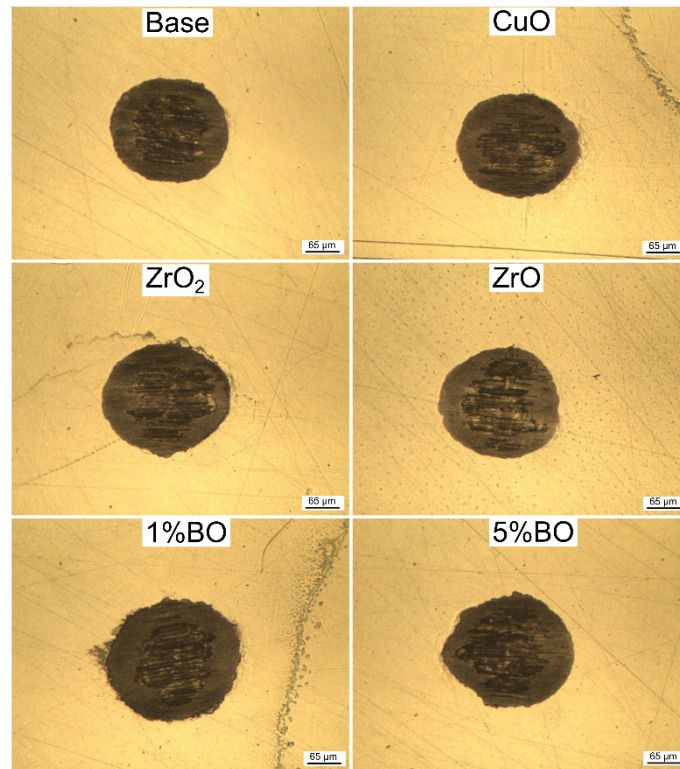


Figure 7. Optical microscopies of lower specimens tested in HFRR rig using 220 cSt grease at 10× magnifications.

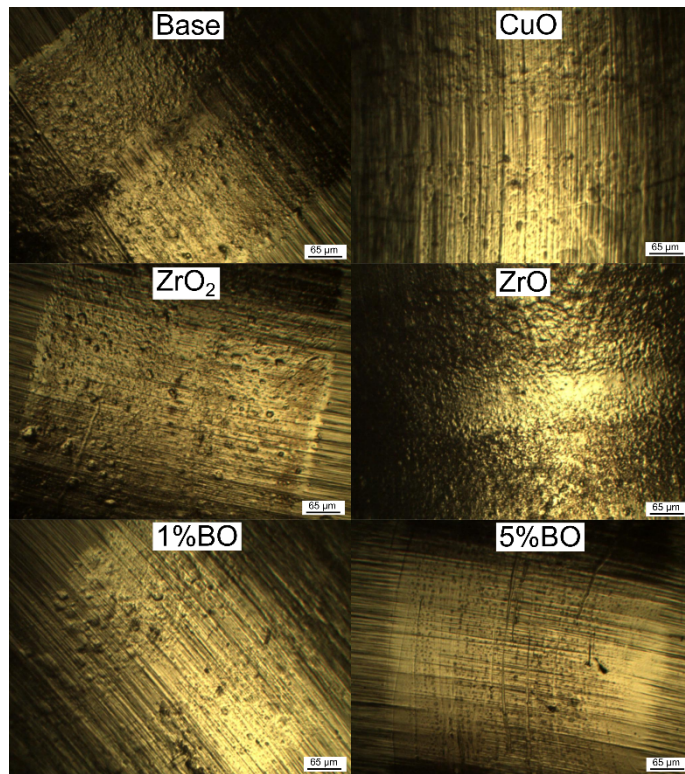


Figure 8. Optical microscopies of thrust bearing raceways tested in modified Fafnir rig using 220 cSt grease at 10× magnifications.

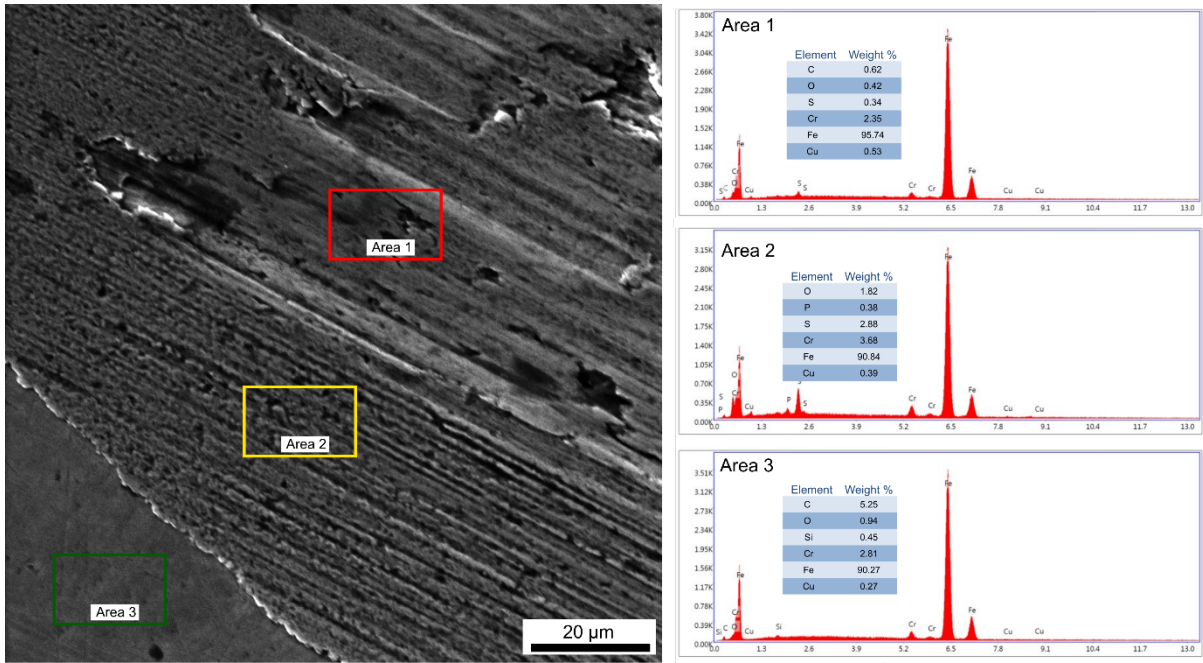


Figure 9. SEM and EDX spectra of lower specimen tested in HFRR rig using 100 + CuO grease at 2130× magnifications.

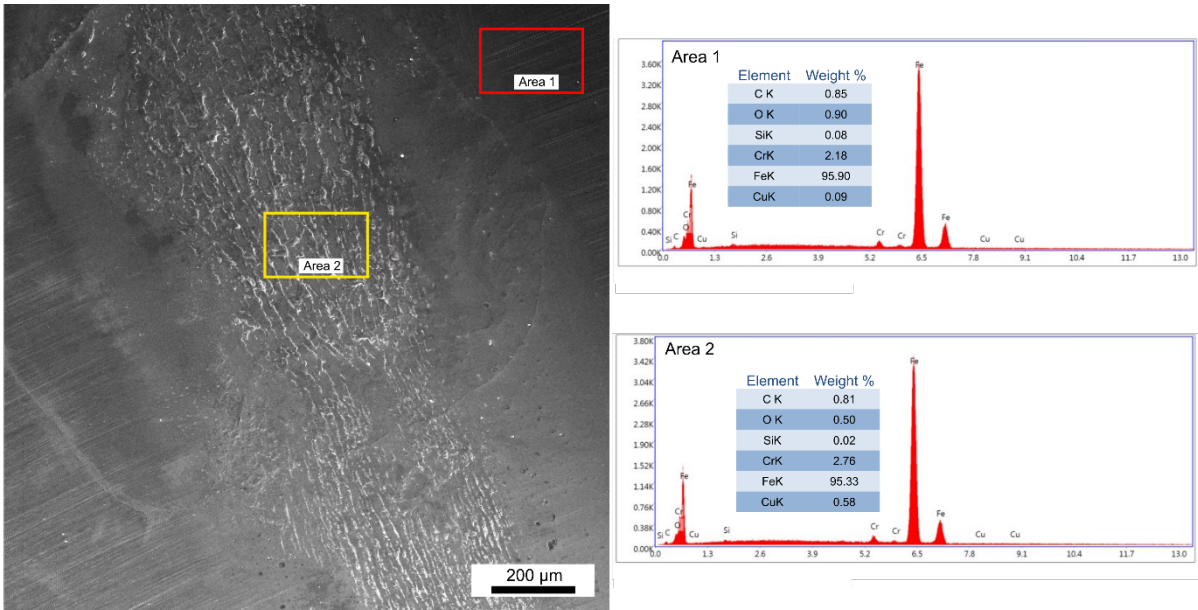


Figure 10. SEM and EDX spectra of thrust bearing raceways tested in modified Fafnir rig using 220 + CuO grease at 140× magnifications.